

# Bell-shaped quadratic spherical cloaks designed by a transformation-free method: Theory and optimization

Andrey Novitsky<sup>1</sup> and Cheng-Wei Qiu<sup>2\*,3</sup>

<sup>1</sup>Department of Theoretical Physics, Belarusian State University, Nezavisimosti Avenue 4, 220050 Minsk, Belarus. Electronic address: andrey.novitsky@tut.by

<sup>2</sup>Research Laboratory of Electronics, Massachusetts Institute of Technology, 77 Massachusetts Avenue, Cambridge, MA 02139, USA.

<sup>3</sup>Department of Electrical and Computer Engineering, National University of Singapore, 4 Engineering Drive 3, Singapore 117576.

E-mail: cwq@mit.edu

**Abstract.** Based on the concept of the cloak generating function, we propose a transformation-free method for the required parameters of spherical cloaks without knowing the needed coordinate transformation beforehand. A non-ideal discrete model is used to calculate and optimize the total scattering cross-sections of different profiles of the generating function. A bell-shaped quadratic spherical cloak is found to be the best candidate, which is further optimized by controlling design parameters involved. Such improved invisibility is steady even when the model is highly discretized.

## 1. Introduction

Recently, great progress has been made in both the theory of and experiments on invisibility cloaks [1, 2, 3, 4]. Wide applications have been found in microwave spectrum [5, 6, 7, 8, 9, 10], optical regime [11, 12, 13, 14, 15, 16], elastodynamics [17, 18], quantum mechanics [19, 20], and acoustics [21, 22, 23, 24]. One approach to achieve an invisibility cloak is to employ the transformation optics (TO) to allow electromagnetic waves to be directed around the concealed region and smoothly recovered afterwards. The anisotropic parameters of such a cloak are derived from the coordinate transformation. This approach was generalized from the cloaking of thermal conductivity [25] and then widely applied in many other areas, which provides new approaches to conceal passive/active objects [26, 27] within their interiors invisible to external illuminations. The fundamental idea is the invariance of Maxwell's equations under a space-deforming transformation if the material properties are altered accordingly; i.e., a specific spatial compression is equivalent to a variation of the material parameters in the flat space. Based on TO concept, many efforts have been devoted to the study of 2D cloaks (cylindrical [31], elliptical [32], and arbitrary cross-section [33]) due to the simplicity in numerical simulations. Inspired by the classic spherical cloak [1], the expressions of electromagnetic fields were explicitly presented in terms of spherical Bessel functions by Mie theory [26]. However, this analytical scattering theory for classic spherical cloaks cannot work if the anisotropic ratio (see the original definition in [34]) is anything other than that in [26]. Two solutions to overcome this problem were proposed: 1) multilayers of alternating isotropic layers [35]; and 2) discrete model of the inhomogeneous anisotropic shell, and each layer is radially anisotropic but homogeneous [36]. Then, the spherical invisibility cloak is near-perfect. Another non-TO route to the cloaking in canonical shape is to use a homogenous anisotropic [28, 29] or isotropic plasmonic [30] coating. However, in this method, the effectiveness and properties of the cloak depend on the object to be cloaked as well as that its size has to be sufficiently small compared with the wavelength. Usually, TO-based spherical cloaks need to know the prescribed transformation functions first and the required parameters can thus be obtained by constructing the explicit transformation matrices. As reported in what follows, there exists an implicit way to derive the needed cloaking parameters, bypassing the traditional procedure mentioned.

In this paper, we propose a new recipe for designing spherical invisibility cloaks, while we do not need to know or use the coordinate transformation throughout. In virtue of the cloak generating function, all parameters of radially anisotropic spherical cloak needs can be determined analytically and uniquely. Nevertheless, the corresponding coordinate transformation can be found by the calculation of those obtained. Therefore, the traditional way to design a cloak is reversed. In addition, this reversed transformation-free method provides us an easy way to investigate the role of the parametric profiles in achieving invisibility. Certainly, those sets of parameters from various generating functions are ideal, all of which should give zero scattering

theoretically. However, in actual situations, one has to consider a discrete multilayered model so that the invisibility performances of different generating functions distinguish from each other. The general method developed in [36] is adopted to calculate the far-field scattering. Our numerical results reveal that the power quadratic bell-shaped cloak yields the lowest scattering under the same discretization, which is still pronounced when the ideal cloaking shell is highly discretized.

This paper is organized as follows. Section 2 proposes the reversed design method based on a transformation-free process, from which the spherical cloak's parameters are determined without knowing specific coordinate transformations. Section 3 addresses that the bell-shaped profile of the generating function outperforms the other including the linear one corresponding to the classic spherical cloak. Section 4 compares different profiles which give rise to bell-shaped profiles. Section 5 discusses the optimization of bell-shaped quadratic cloaks where the steady improvement in invisibility performance is verified.

## 2. Transformation-Free Design Method for Arbitrary Spherical Cloaks

We consider that the parameters of the spherical cloak only dependent upon the radial position of the spherical coordinates. Supposing  $r'$  as radial coordinate in virtual space and  $r$  as that of the physical space, one concludes that dielectric permittivity and magnetic permeability tensors, in terms of impedance matching, are

$$\varepsilon(r) = \mu(r) = \begin{pmatrix} \varepsilon_r(r) & 0 & 0 \\ 0 & \varepsilon_t(r) & 0 \\ 0 & 0 & \varepsilon_t(r) \end{pmatrix} = \begin{pmatrix} \lambda_r/\lambda_t^2 & 0 & 0 \\ 0 & 1/\lambda_r & 0 \\ 0 & 0 & 1/\lambda_r \end{pmatrix}, \quad (1)$$

where  $\varepsilon_r(r)$  and  $\varepsilon_t(r)$  are the radial and transverse dielectric permittivities (they coincide with radial and transverse magnetic permeabilities), and

$$\lambda_r = \frac{dr}{dr'}, \quad \lambda_t = \frac{r}{r'}. \quad (2)$$

From the above expressions we derive a set of equations

$$\frac{dr}{dr'} = \frac{1}{\varepsilon_t(r)}, \quad \frac{r}{r'} = \frac{1}{\sqrt{\varepsilon_r(r)\varepsilon_t(r)}}. \quad (3)$$

Manipulating Eq. (3), we arrive at a differential equation to relate radial and transverse permittivities as

$$\frac{d(r\sqrt{\varepsilon_r(r)\varepsilon_t(r)})}{dr} = \varepsilon_t(r). \quad (4)$$

It should be noted that Eq. (4) is transformation-free, which only directly displays the expression dielectric permittivities of a spherical cloak has to satisfy. This approach is an inverse approach. The direct method is to find the dielectric permittivities from a known function of coordinate transformation. The inverse approach derives the coordinate

transformation from the known radial and transverse dielectric permittivities. Eq. (4) can be easily integrated:

$$r\sqrt{\varepsilon_t(r)\varepsilon_r(r)} = C + \int_a^r \varepsilon_t(r_1)dr_1, \quad (5)$$

where  $C$  is the integration constant. The left-hand side of Eq. (5) is identical to  $r'$  as suggested in Eq. (3). Hence, there are still two boundary conditions to be used. From the first boundary condition ( $r' = 0$  at  $r = a$ ) we can determine the integration constant:  $C = 0$ . From the second boundary condition ( $r' = b$  at  $r = b$ ) we obtain the normalization condition for the transverse dielectric permittivity

$$b = \int_a^b \varepsilon_t(r_1)dr_1. \quad (6)$$

Normalization can be taken into account automatically using the cloak generating function  $g(r)$  which is proportional to the transverse dielectric permittivity (i.e.,  $g(r) = C_0\varepsilon_t(r)$  and  $C_0$  is a constant which will be automatically canceled). Then transverse dielectric permittivity can be presented in the form

$$\varepsilon_t(r) = \frac{bg(r)}{\int_a^b g(r_1)dr_1}. \quad (7)$$

Radial dielectric permittivity can be expressed from Eq. (5) as

$$\varepsilon_r = \frac{b(\int_a^r g(r_1)dr_1)^2}{r^2g(r)\int_a^b g(r_1)dr_1}. \quad (8)$$

We will further classify spherical cloaks in terms of the generating function  $g(r)$ . Pendry's classic spherical cloak corresponds to the constant generating function  $g(r) = 1$ : substituting  $g(r) = 1$  into Eqs. (7) and (8) one can easily derive transverse dielectric permittivity  $\varepsilon_t = b/(b - a)$  and radial dielectric permittivity  $\varepsilon_r = b(r - a)^2/r^2(b - a)$ . There are many non-trivial cloak designs, e.g. linear, quadratic, cubic, sinusoidal, etc., which will be studied in this paper.

### 3. Bell-Shaped Generating Function for Cloak Optimization

Starting from this section we consider non-ideal cloaks since we use a discrete model to compute and compare the far-field scattering. If the ideal cloaks are considered, each of the cloak design is equivalent leading to zero scattering. Realistic cloaks can be made of multiple homogeneous spherical layers, which replace the inhomogeneous cloaking shell. In this case the scattering is not zero, but noticeably reduced, and such a cloak realization is called non-ideal (see Fig. 1). In this section we will find the best non-ideal cloak providing the lowest cross-section among all designs investigated.

We will consider some typical generating functions (for transverse dielectric permittivities) which exhibit different types of profiles. The simplest generating functions are constant, linear, and quadratic ones. Which of them provides the best cloaking performance?

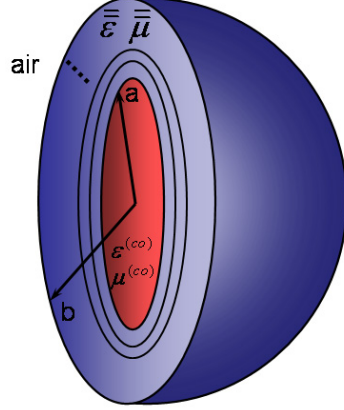


**Figure 1.** Illustration of the cloaking shell covering the object to be concealed. We consider the spherical cloak in free space with the inner radius  $k_0 a = \pi$  and outer radius  $k_0 b = 2\pi$ . The core material is glass ( $\varepsilon^{(co)} = 1.45^2$  and  $\mu^{(co)} = 1$ ). These quantities are used throughout the whole paper. The material parameters  $\bar{\varepsilon}$  and  $\bar{\mu}$  are determined by applying the proposed transformation-free method to an arbitrary cloaking generating function. The cloaking shell is equally divided into  $N$  layers (each layer is homogeneous and anisotropic), and the scattering theory in [36] is used to compute the far-field diagrams.

Constant generating function produces the dielectric permittivities of the Pendry's classic spherical cloak as it has been demonstrated in the previous section. Linear generating function can be generally written as  $g(r) = r - p$ , where  $p$  is a constant parameter. In this case transverse (7) and radial (8) dielectric permittivities become

$$\varepsilon_t(r) = \frac{2b(r-p)}{(b-a)(b+a-2p)}, \quad (9)$$

$$\varepsilon_r = \frac{b(r-a)^2(r+a-2p)^2}{2r^2(r-p)(b-a)(b+a-2p)}. \quad (10)$$

Parameter  $p$  can take any value except  $(a+b)/2$ . It controls the slope of the transverse permittivity function. If  $p < (a+b)/2$ ,  $\varepsilon_t(r)$  linearly increases, and otherwise it monotonically decreases.

Quadratic generating function has the general form  $g(r) = (r-p)(r-d) + s$ , where  $p$ ,  $d$ , and  $s$  are tunable parameters. The expressions for the permittivities in quadratic case can be deduced to

$$\varepsilon_t(r) = \frac{b[(r-p)(r-d) + s]}{P(b)}, \quad (11)$$

$$\varepsilon_r = \frac{bP^2(r)}{r^2[(r-p)(r-d) + s]P(b)}, \quad (12)$$

where

$$P(r) = \frac{r^3 - a^3}{3} - (p+d)\frac{r^2 - a^2}{2} + (pd + s)(r - a). \quad (13)$$

Quadratic transverse permittivity is a parabola in graphical presentation. The parabola can have a minimum (i.e.,  $s > s_0$ ) or maximum (i.e.,  $s < s_0$ ), where  $s_0 = -(b^2 + ab +$

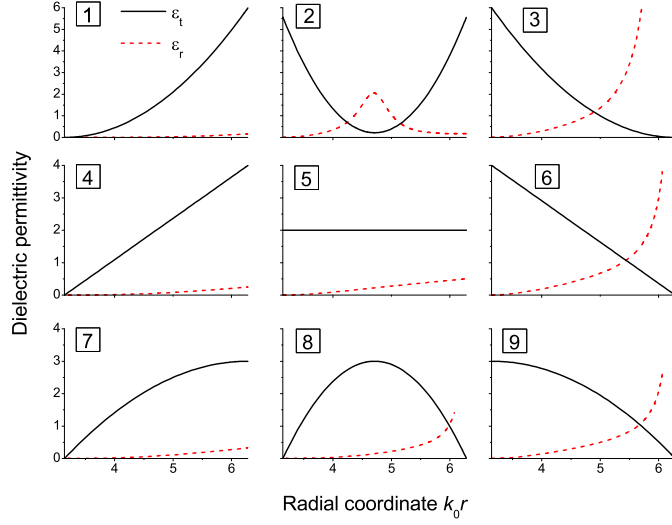


**Figure 2.** Transverse  $\varepsilon_t$  and radial  $\varepsilon_r$  dielectric permittivities corresponding to different profiles of generating function. Profiles 1–9 are described as follows: (1) quadratic generating function with  $p = 0$ ,  $d = b$ ,  $s = b^2/4$ ; (2) quadratic generating function with  $p = a$ ,  $d = b$ ,  $s = (b - a)^2/4 + 0.1$ ; (3) quadratic generating function with  $p = a$ ,  $d = 2b - a$ ,  $s = (b - a)^2$ ; (4) linear generating function with  $p = a$ ; (5) constant generating function; (6) linear generating function with  $p = b$ ; (7) quadratic generating function with  $p = a$ ,  $d = 2b - a$ ,  $s = 0$ ; (8) quadratic generating function with  $p = a$ ,  $d = b$ ,  $s = 0$ ; (9) quadratic generating function with  $p = 0$ ,  $d = b$ ,  $s = 0$ .

$$a^2)/3 + (p + d)(a + b)/2 - pd.$$

Using these generating functions, some typical situations depicted in Fig. 2 are presented. Profile 5 demonstrates the permittivities for the constant generating function  $g(r) = 1$  corresponding to Pendry's cloak. Linear generating functions are presented in Profile 4 ( $g(r) = r - a$ ) and Profile 6 ( $g(r) = r - b$ ). The other profiles are produced using quadratic generating functions.

The performances of different cloaks can be compared in terms of their scattering cross-sections. The best cloaking design possesses the lowest cross-section because of the reduced interaction of the electromagnetic wave with the spherical particle. The inhomogeneous anisotropic spherical cloaking shell is divided into  $N$  homogeneous anisotropic spherical layers. An experimental realization of this multilayer cloak can be the sputtering onto the spherical core. Throughout the whole paper we use  $N = 30$ .

In Fig. 3 the total cross-sections resulting from different generating functions are shown. Some profiles are approximately equivalent, for example, 1, 2 and 3, or 4 and 6, or 7 and 9. Profiles 1–3 are characterized by concave-up transverse dielectric permittivity  $\varepsilon_t'' > 0$ . According to Fig. 3 they give rise to the worst results. The flat-curvature profiles 4–6 characterized by  $\varepsilon_t'' = 0$  are much better. Pendry's cloak (number 5) stands out against the other zero-curvature profiles. However, the most effective cloak design is the case of concave-down transverse permittivity  $\varepsilon_t'' < 0$ . Profiles 7, 8, and 9 are better than profiles 4, 5, and 6, respectively, by approximately 4.8 dB. The quadratic cloak

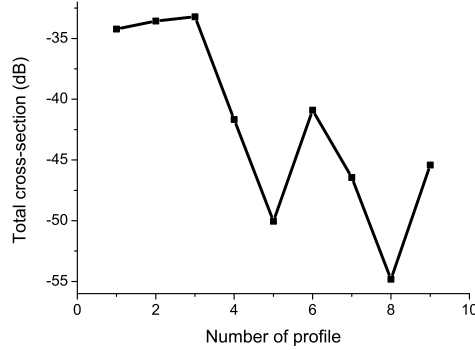


**Figure 3.** Total cross-sections for profiles of permittivities shown in Fig. 2. The number of discrete layers forming the cloak equals  $N = 30$ .

with concave-down transverse permittivity (bell-shaped cloak) is shown to be the best candidate.

The maximum of  $\varepsilon_t$  in profile 8 is in the middle position of the cloaking shell. Shifting the maximum of such a bell shape towards the limit at the outer boundary (i.e., profile 7) or inner boundary (i.e., profile 9), the cloaking performance is monotonically degraded as shown in Fig. 3. If parameter  $s$  is extremely huge in quadratic generating function ( $s \rightarrow \infty$ ), the cloak permittivities coincide with those of Pendry's cloak. Thus, the increase of  $s$  improves the cloak 2 and deteriorates the cloak 8.

#### 4. The General Class of Bell-Shaped Cloaks

From the previous section it is concluded that the bell-shaped profile of the transverse dielectric permittivity leads to the optimal non-ideal cloaking performance. In the present section we will consider the general class of bell-shaped cloaks and choose the best type.

Apart from the quadratic cloak, another three simple bell-shaped profiles will be considered: Gaussian, Lorentzian, and Sech. All of them have a single parameter  $T$ , which sets the width of the profile. We take the maxima of such transverse permittivities in the middle of the cloaking shell region (at the point  $(a + b)/2$ ) to compare with quadratic cloak.

Gaussian cloak has the generating function  $g(r) = \exp[-(r - (a + b)/2)^2/(4T^2)]$ . The permittivity functions are

$$\begin{aligned} \varepsilon_t &= \frac{b}{2\sqrt{\pi}T\text{Erf}[(b-a)/(4T)]} e^{-\frac{(r-(a+b)/2)^2}{4T^2}} \\ \varepsilon_r &= \frac{\sqrt{\pi}Tb(\text{Erf}[(b+a-2r)/(4T)] - \text{Erf}[(b-a)/(4T)])^2}{2r^2\text{Erf}[(b-a)/(4T)]} e^{\frac{(r-(a+b)/2)^2}{4T^2}}. \end{aligned} \quad (14)$$

The generating function of the Lorentzian cloak is  $g(r) = 1/[1 + (r - (a + b)/2)^2/T^2]$ .

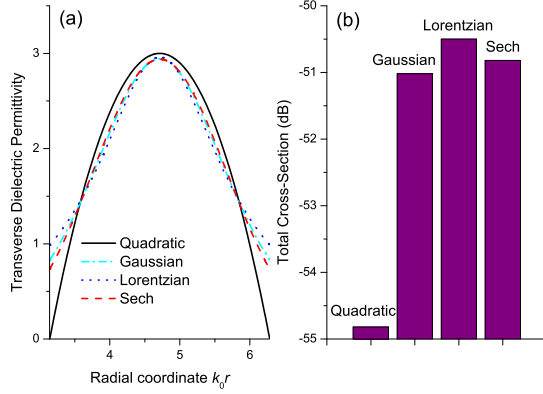


**Figure 4.** (a) Profiles of transverse dielectric permittivity for quadratic (profile No. 8 in Fig. 2), Gaussian, Lorentzian, and Sech cloaks and (b) total cross-sections of these cloaks. Parameter  $T$  equals  $(b-a)/4\sqrt{2}\ln 2$  for Gaussian,  $(b-a)/(2\sqrt{2})$  for Lorentzian, and  $(b-a)/(2\sqrt{2}\ln(\sqrt{2}+1))$  for Sech cloak. The number of discrete layers forming the cloak equals  $N = 30$ .

The transverse and radial permittivities for this cloak are of the form

$$\begin{aligned} \varepsilon_t &= \frac{b}{2T[1 + (r - (a+b)/2)^2/T^2] \arctan[(b-a)/(2T)]} \\ \varepsilon_r &= \frac{Tb(\arctan[(b+a-2r)/(2T)] - \arctan[(b-a)/(2T)])^2}{2r^2 \arctan[(b-a)/(2T)]} \times \\ &\quad \left(1 + \frac{(r - (a+b)/2)^2}{T^2}\right). \end{aligned} \quad (15)$$

Sech cloak generating function depends on the radial coordinate as  $g(r) = \text{sech}^2[(r - (a+b)/2)/T]$ . The permittivities are as follows

$$\begin{aligned} \varepsilon_t &= \frac{b \text{sech}^2[(r - (a+b)/2)/T]}{2T \tanh[(b-a)/(2T)]} \\ \varepsilon_r &= \frac{Tb(\tanh[(2r - b - a)/(2T)] - \tanh[(b-a)/(2T)])^2}{2r^2 \text{sech}^2[(r - (a+b)/2)/T] \tanh[(b-a)/(2T)]}. \end{aligned} \quad (16)$$

We choose equal 3 dB bandwidths for various transverse permittivity profiles to compare different cloaks. Parameters  $T$  which are tuned to provide identical 3 dB bandwidth for each cloak are given in the caption of Fig. 4. In this figure we show the total cross-sections of quadratic, Gaussian, Lorentzian, and Sech cloaks. Profiles of Gaussian, Lorentzian, and Sech cloaks are very close, resulting in similar scattering cross-sections. The influence of the permittivity functions on the cloak performance is difficult to tell among these three cloaks. However, it is shown that quadratic cloak in Fig. 4 provides better invisibility when its transverse permittivity vanishes at the inner and outer boundaries of the cloaking shell.

Since the shapes of the Gaussian, Lorentzian, and Sech cloaks are similar, we can just select one of them, (e.g., Gaussian) to investigate the significance of the profile, which can be varied by the parameter  $T$ . The results are demonstrated in Fig. 5.

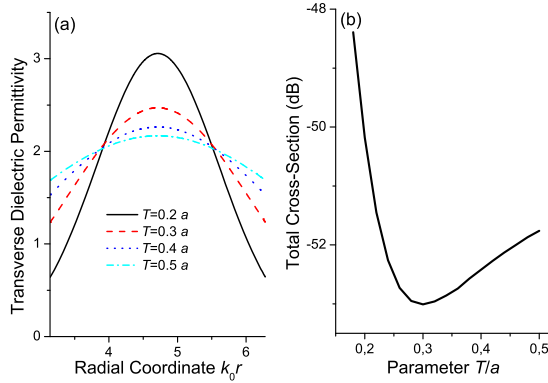


**Figure 5.** (a) Profiles of transverse dielectric permittivity for Gaussian cloaks with different parameters  $T$  and (b) total cross-sections versus parameter  $T$ . The number of discrete layers forming the cloak equals  $N = 30$ .

The total cross-section has a minimum, which does not provide better cloaking than quadratic one though. The cross-section minimization is achieved approximately at  $T = 0.3a$ . This profile is shown in Fig. 5(a) along with profiles for other  $T$  parameters. According to this figure the minimization profile has the 3 dB bandwidth equal  $(b-a)/2$ . Such a profile is neither too narrow nor too wide because narrow profiles ( $T \rightarrow 0$ ) need extremely high discretization and wide profiles ( $T \rightarrow \infty$ ) tend to the limit of Pendry's cloak as shown in Fig. 5(b).

Thus the bell-shaped quadratic cloak is preferred for non-ideal cloak design, which has the lowest cross-section among all bell-shaped cloaks considered in this section. In the following section we will show how the quadratic cloak results can be improved.

## 5. Improved Quadratic Cloaks

Quadratic cloak is characterized by very simple profile of the transverse dielectric permittivity. Also, the quadratic cloak has the scattering almost 5 dB lower than that of classic spherical one. Our aim of this section is to find a way of creating the high-performance cloaks based on the transformation-free design method and bell-shaped quadratic cloak. The high-performance cloak should be similar to the quadratic one. Transverse permittivity should have a maximum and vanish at the inner and outer radii of the shell:  $\varepsilon_t(a) = \varepsilon_t(b) = 0$ . These properties can be satisfied for general generating function of the form

$$g(r) = (r - a)(r - b)g_1(r). \quad (17)$$

By choosing function  $g_1(r)$ , we can set the permittivity profile of the cloak. The function  $g_1(r)$  can take arbitrary values at the cloak edges  $r = a$  and  $r = b$ , though it should provide the maximum of the transverse permittivity. At first we will consider the maximum at the center of the cloak  $r = (a+b)/2$ , and then the effect of the non-central maximum position will be studied. For instance function  $g_1(r)$  can be selected with

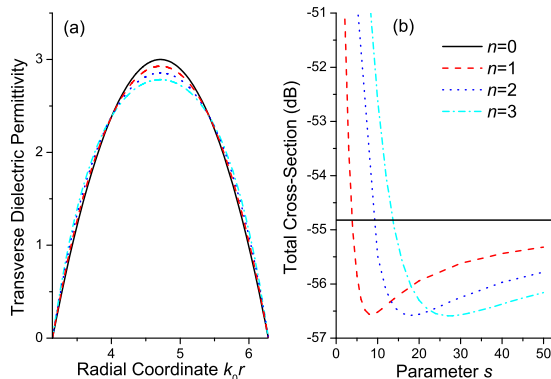


**Figure 6.** (a) Profiles of transverse permittivity for power quadratic cloaks and (b) total cross-sections of these cloaks versus parameter  $s$ . Parameters:  $p = a$ ,  $d = b$ ,  $N = 30$ . In (b), only  $s > 0$  is considered for cloaking purposes because the total cross-sections corresponding to  $s < 0$  are significantly larger.

Gaussian profile. Then the cloak can be called Gaussian-quadratic one. However, such a design is worse than the simple quadratic shape. To provide the better design we will focus the quadratic dependence using the  $g_1(r)$  function

$$g_1(r) = ((r - p)(r - d) + (d - p)^2/4 + s)^n. \quad (18)$$

When  $n = 0$ , it is just the bell-shaped quadratic cloak discussed before. The permittivities at  $n > 0$  are suppressed due to lengthy expressions.

In the generating function set by Eqs. (17) and (18) we can vary the power term  $n$  (the curvature of the transverse permittivity profile at peak), parameters  $s$  (the deviation from the quadratic cloak) and  $d$  (the deviation of the permittivity peak from the center of the cloaking region). At  $n = 0$  the generating function is independent on  $s$  and  $d$  so the total cross-section is the straight line in Fig. 6 (the solid line), where other positive values of  $n$  are shown as well. The minima of the cross-sections (the best cloaking performance) occurs to the parameter  $s$  approximately at  $s_{min} \approx 9n$ , i.e., linear to the power  $n$ . At larger parameter  $s$ , the curves tend to the cross-section of the quadratic cloak. At small and negative  $s$ , the shape of the transverse permittivity contains the minimum and a couple of maxima, therefore the total cross-section is substantially increased. In Fig. 6(b), the cloaking performance is obviously improved compared with the quadratic cloak. Let us further study the effect of the peak position of the profile, which is controlled by the parameter  $d$ .

The case  $d = b$  describes that the position of the permittivity maximum is in the center of the cloaking shell region. If  $d < b$  ( $d > b$ ), the maximum is shifted towards the outer (inner) radius of the cloaking shell. Fig. 7 shows that the central position of the permittivity maximum is not the optimal choice. The minimization of the cross-section is achieved for  $d \approx 0.84b$ . Such a non-central position is expected to result from the spherically curvilinear geometry of the cloak.

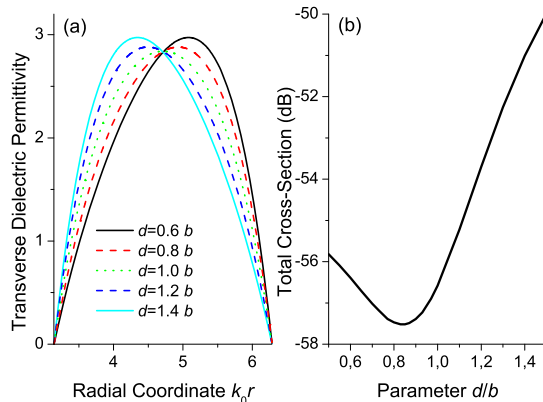


**Figure 7.** (a) Profiles of transverse dielectric permittivity for power quadratic cloaks and (b) total cross-sections of these cloaks vs. parameter  $d$ . Parameters:  $p = a$ ,  $n = 2$ ,  $s = 18$ ,  $N = 30$ .

Compared with the quadratic cloak, the improvement of the performance of power quadratic cloak is considerable: the total cross-section is further decreased from  $-54.84$  dB to  $-57.52$  dB. The improvement is caused by the shape of the profile. The profile should be parabolic-like with a slightly deformed shape.

It is also important to consider the differential cross-sections which provides the scattering intensity at an arbitrary angle. In Fig. 8 we show the differential cross-sections for some typical cloaking designs designed by the transformation-free method and considered in a non-ideal situation. The common feature of the cloaks is the reduced backscattering. It is seen that the classic spherical cloak is the most visible one. The quadratic cloak (blue dotted line) can provide much lower scattering over almost all angles compared with Pendry's and Gaussian's bell-shaped cloak. The power quadratic cloak is able to further bring down the scattering of the quadratic cloak near the forward direction.

However, one may question that our non-ideal situation may approach to the ideal case when the discretization is high (i.e.,  $N$  is much larger than 30). If so, each cloak derived from our proposed reversed algorithm should be more and more identical to each other. Theoretically, it is true provided that  $N \rightarrow \infty$ , while the influence of the discretization number  $N$  on the optimization result is still of significant importance in practice. We calculate the total cross-sections for different numbers of spherical layers in Fig. 9. In general, we observe the conservation of our conclusions on the optimization for  $N = 30$ , except for that the performance of the Gaussian cloak matches with that of the quadratic cloak at  $N = 70$ . When  $N$  is small, the dependence of scattering reduction on the value of  $N$  is nonlinear. For great number of layers  $N$  the curves become mostly linear as shown in Fig. 9.

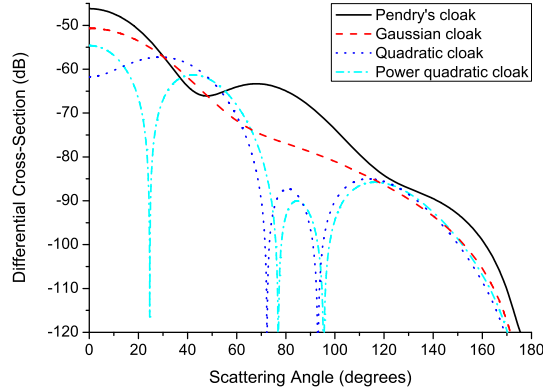


**Figure 8.** Differential cross-sections of the cloaks derived by the proposed transformation-free method. The cloak parameters of each given design have been selected to provide the best performance respectively. Parameters:  $T = 0.3a$  for Gaussian cloak;  $s = 18$ ,  $n = 2$ ,  $p = a$ , and  $d = 0.84b$  for power quadratic cloak;  $N = 30$ .

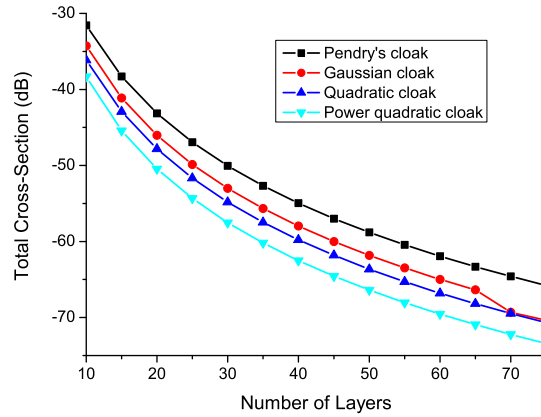


**Figure 9.** Total cross-sections of different cloak designs versus the number of spherical layers  $N$ . Parameters of the cloaks are the same as those in Fig. 8.

## 6. Conclusion

We have proposed a transformation-free method to obtain required parameters of a spherical cloak, based on the concept of the cloaking generating function. It has been found that the bell-shaped cloaks provide the smallest interaction of the cloaking shell with the electromagnetic radiation under the non-ideal situation (i.e., the cloaking shell is discretized into  $N$  layers). Among the bell-shaped cloaks, we have compared quadratic, Gaussian, Lorentzian, and Sech cloaks. The last three are very similar in profile shape and dependence of controlling parameters. We have concluded that the best performance is achieved when the bell-shaped transverse permittivity profiles which vanish at the inner and outer radii of the cloaking shell. The simplest design of such a type is the quadratic cloak. Improved invisibility performance can be provided by

the power quadratic cloak with the maximum of the permittivity profile slightly shifted towards the outer boundary. The decrease of cloak's overall scattering is about 7.5 dB compared with the classical Pendry's design, and the improvement is steady even when the discretization  $N$  is quite high.

## Acknowledgement

This research was supported in part by the Army Research Office through the Institute for Soldier Nanotechnologies under Contract No. W911NF-07-D-0004. A. Novitsky acknowledges the Basic Research Foundations of Belarus (F08MS-06). We thank Prof. John Joannopoulos and Prof. Steven Johnson for their stimulating comments and revisions throughout the manuscript preparation.

## References

- [1] Pendry J B, Schurig D and Smith D R 2006 *Science* **312** 1780
- [2] Leonhardt U *Science* 2006 **312** 1777
- [3] Schurig D, Mock J J, Justice B J, Cummer S A, Pendry J B, Starr A F and Smith D R 2006 *Science* **314** 977
- [4] Liu R, Ji C, Mock J J, Chin J Y, Cui T J and Smith D R 2009 *Science* **323** 366-369
- [5] Leonhardt U 2006 *New J. Phys.* **8** 118
- [6] Miller D A B 2006 *Opt. Express* **14** 12457
- [7] Schurig D, Pendry J B and Smith D R 2006 *Opt. Express* **14** 9794
- [8] Nicorovici N A P, Milton G W, McPhedran R C and Botten L C 2007 *Opt. Express* **15** 6314
- [9] Liang Z X, Yao P J, Sun X W and Jiang X Y 2008 *Appl. Phys. Lett.* **92** 131118
- [10] Zhao Y, Argyropoulos C and Hao Y 2008 *Opt. Express* **16** 6717
- [11] Cai W S, Chettiar U K, Kildishev A V and Shalaev V M 2007 *Nat. Photonics* **1** 224
- [12] Cai W S, Chettiar U K, Kildishev A V and Shalaev V M 2008 *Opt. Express* **16** 5444
- [13] Vanbesien O, Fabre N, Melique X and Lippens D 2008 *Appl. Opt.* **47** 1358
- [14] Xiao D and Johnson H T 2008 *Opt. Lett.* **33** 860
- [15] Jenkins A 2008 *Nat. Photonics* **2** 270
- [16] Valentine J, Li J, Zentgraf T, Bartal G and Zhang X 2009 *Nat. Mater.* doi:10.1038/nmat2461
- [17] Milton G W, Briane M and Willis J R 2006 *New J. Phys.* **8** 248
- [18] Farhat M, Guenneau S, Enoch S and Movchan A B 2009 *Phys. Rev. B* **79** 033102
- [19] Zhang S, Genov D A, Sun C and Zhang X 2008 *Phys. Rev. Lett.* **100** 123002
- [20] Greenleaf A, Kurylev Y, Lassas M and Uhlmann G 2008 *Phys. Rev. Lett.* **101** 220404
- [21] Chen H and Chan C T 2007 *Appl. Phys. Lett.* **91** 183518
- [22] Cummer S A and Schurig D 2007 *New J. Phys.* **9** 45
- [23] Cai L W and Sanchez-Dehesa J 2007 *New J. Phys.* **9** 450
- [24] Cummer S A, Popa B I, Schurig D, Smith D R, Pendry J, Rahm M and Starr A 2008 *Phys. Rev. Lett.* **100** 024301
- [25] Greenleaf A, Lassas M and Uhlmann G 2003 *Physiol. Meas.* **24** 413
- [26] Chen H, Wu B I, Zhang B and Kong J A 2007 *Phys. Rev. Lett.* **99** 063903
- [27] Zhang B, Chen H, Wu B I and Kong J A 2008 *Phys. Rev. Lett.* **100** 063904
- [28] Gao L, Fung T H, Yu K W and Qiu C W 2008 *Phys. Rev. E* **78** 046609
- [29] Ni Y X, Gao L and Qiu C W 2009 Preprint 0905.1503 [physics.optics]
- [30] Alu A and Engheta N 2007 *Opt. Express* **15** 3318
- [31] Kwon D and Werner D H 2008 *Appl. Phys. Lett.* **92** 013505

- [32] Jiang W X, Cui T J, Yu G X, Lin X Q, Cheng Q and Chin J Y 2008 *J. Phys. D: Appl. Phys.* **41** 085504
- [33] Nicolet A, Zolla F and Guenneau S 2008 *Opt. Lett.* **33** 1584
- [34] Qiu C W, Li L W, Yeo T S and Zouhdi S 2007 *Phys. Rev. E* **75** 026609
- [35] Qiu C W, Hu L, Xu X and Feng Y 2009 *Phys. Rev. E* **79** 047602
- [36] Qiu C W, Novitsky A, Ma H and Qu S 2009 Preprint 0905.1703 [physics.optics]